

Hrq1, a Homolog of the Human RecQ4 Helicase, Acts Catalytically and Structurally to Promote Genome Integrity

Matthew L. Bochman,^{1,2,3,*} Katrin Paeschke,^{1,2,4} Angela Chan,¹ and Virginia A. Zakian¹

¹Department of Molecular Biology, Princeton University, Princeton, NJ 08544, USA

²These authors contributed equally to this work

³Present address: Molecular and Cellular Biochemistry Department, Indiana University, Bloomington, IN 47405, USA

⁴Present address: Department of Biochemistry, Theodor Boveri-Institute, University of Würzburg, Am Hubland, 97074 Würzburg, Germany

*Correspondence: bochman@indiana.edu

<http://dx.doi.org/10.1016/j.celrep.2013.12.037>

This is an open-access article distributed under the terms of the Creative Commons Attribution-NonCommercial-No Derivative Works License, which permits non-commercial use, distribution, and reproduction in any medium, provided the original author and source are credited.

SUMMARY

Human RecQ4 (hRecQ4) affects cancer and aging but is difficult to study because it is a fusion between a helicase and an essential replication factor. Budding yeast Hrq1 is homologous to the disease-linked helicase domain of RecQ4 and, like hRecQ4, is a robust 3'-5' helicase. Additionally, Hrq1 has the unusual property of forming heptameric rings. Cells lacking Hrq1 exhibited two DNA damage phenotypes: hypersensitivity to DNA interstrand crosslinks (ICLs) and telomere addition to DNA breaks. Both activities are rare; their coexistence in a single protein is unprecedented. Resistance to ICLs requires helicase activity, but suppression of telomere addition does not. Hrq1 also affects telomere length by a noncatalytic mechanism, as well as telomerase-independent telomere maintenance. Because Hrq1 binds telomeres *in vivo*, it probably affects them directly. Thus, the tumor-suppressing activity of RecQ4 could be due to a role in ICL repair and/or suppression of *de novo* telomere addition.

INTRODUCTION

Helicases are motor proteins that use the energy of nucleotide hydrolysis to separate duplex nucleic acids into their component single strands (Abdelhaleem, 2010). RecQ family helicases are involved in many aspects of DNA replication, recombination, and repair (Bernstein et al., 2010). Humans encode five RecQs (hRecQ1, hBLM, hWRN, hRecQ4, and hRecQ5), and mutations in three of these enzymes (hBLM, hWRN, and hRecQ4) are linked to cancers and/or premature aging. This article presents *in vitro* and *in vivo* studies of the *Saccharomyces cerevisiae* Hrq1 helicase, a homolog of hRecQ4.

Mutation of hRecQ4 is linked to three distinct diseases with related and overlapping symptoms and which are all characterized by genome instability, premature aging, and increased

cancer risk (Capp et al., 2010; Larizza et al., 2010). However, determining how loss of hRecQ4 promotes human disease is complicated because its N terminus is homologous to the essential *S. cerevisiae* Sld2 DNA replication factor (Figure 1A) (Liu, 2010). Given that 95% of the known disease-causing alleles of hRecQ4 are found C-terminal to its Sld2-like domain (Larizza et al., 2010), these diseases are probably due to loss of its helicase activities rather than loss of its replication function, which would presumably be lethal. Thus, a simple model to determine the nonreplication functions of RecQ4 would be useful.

Fungi such as *S. cerevisiae* and *Schizosaccharomyces pombe* were previously described as encoding only one RecQ helicase (Sgs1 and Rqh1, respectively) that is functionally homologous to hBLM (Mirzaei et al., 2011). However, computational analyses recently identified the product of the *S. cerevisiae* YDR291W gene as a homolog of hRecQ4 (Lee et al., 2005) and found similar RecQ4 homologs in many fungal and plant genomes, naming these proteins Hrq1 (Barea et al., 2008).

Here, we purified *S. cerevisiae* Hrq1 and showed that it is a 3'-5' DNA helicase. Mutation of the *S. cerevisiae* HRQ1 resulted in strong sensitivity to DNA interstrand crosslinks (ICLs), a phenotype also reported for hRecQ4-deficient fibroblasts (Jin et al., 2008). In addition, Hrq1, like other RecQ helicases, had multiple telomere functions. HRQ1 suppressed telomere addition (TA) to DSBs, an activity it shares with Pif1, a yeast DNA helicase whose human counterpart is proposed to be a tumor suppressor gene (Chisholm et al., 2012). HRQ1 also suppressed telomere hyperelongation in *pif1* mutant cells. However, unlike Pif1, which acts catalytically at both DSBs and telomeres (Boulé et al., 2005; Myung et al., 2001a; Zhou et al., 2000), neither of these telomeric functions required the helicase activity of Hrq1. Like hBLM (Stavropoulos et al., 2002) and Sgs1 (Huang et al., 2001; Johnson et al., 2001), Hrq1 was also important for telomerase-independent telomere maintenance.

RESULTS

Purified Hrq1 Displays Robust Helicase Activity

To compare the biochemical functions of Hrq1 and RecQ4, full-length *S. cerevisiae* Hrq1 and hRecQ4, as well as catalytically

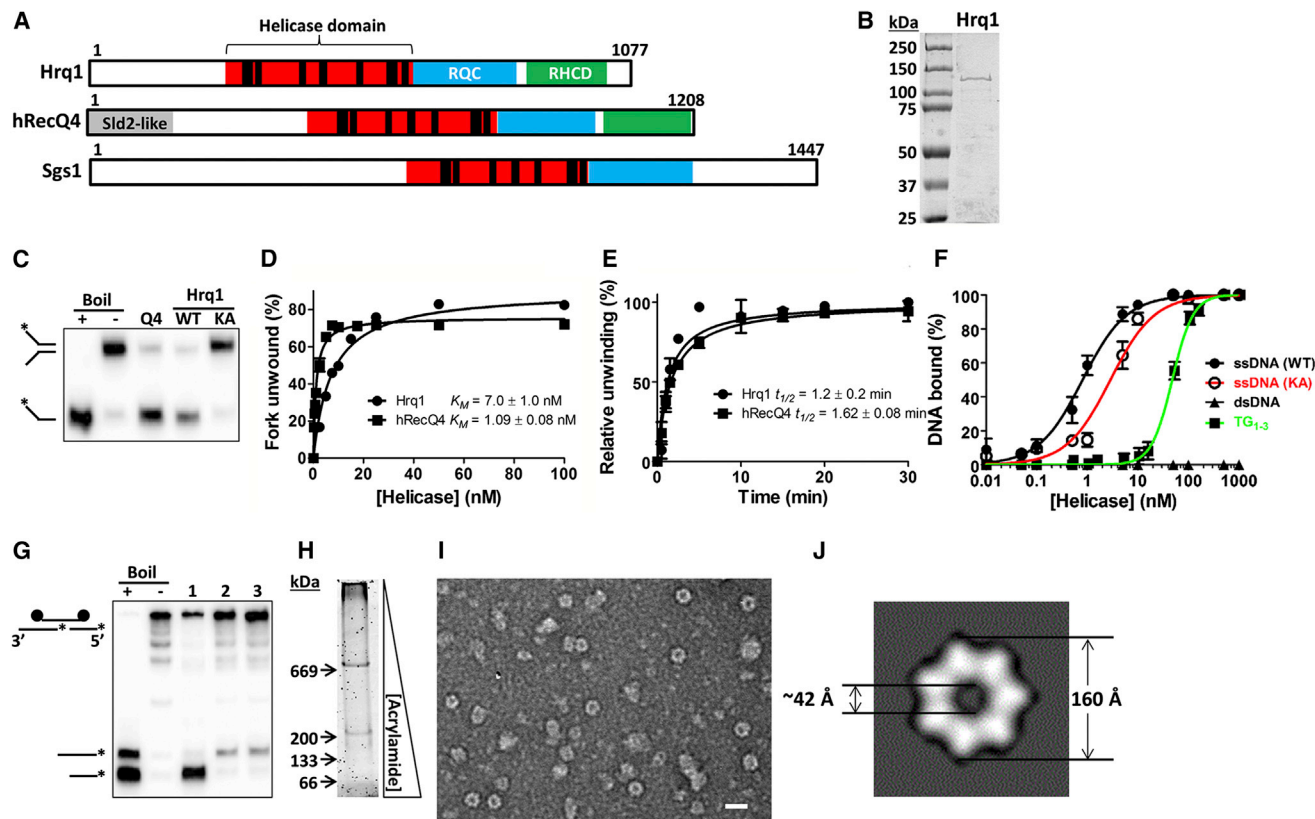


Figure 1. Purified Hrq1 Is an Active 3'-5' Helicase

(A) Domain schematics of Hrq1, hRecQ4, and Sgs1. The amino acid length of each is given on the right. The black bars in the helicase domain correspond to conserved ATPase/helicase motifs. RQC, RecQ C-terminal domain; RHCD, RecQ4/Hrq1-conserved domain; Sld2-like, portion of hRecQ4 homologous to *S. cerevisiae* Sld2.

(B) Coomassie-stained gel of purified *S. cerevisiae* Hrq1. The expected molecular weight is ~130 kDa.

(C) hRecQ4 (Q4) and Hrq1 (WT) (both 50 nM) unwind a fork substrate; 100 nM Hrq1-KA (KA) does not.

(D) Hrq1 and hRecQ4 unwind the fork with similar apparent K_M s ([protein] necessary to unwind 50% of the DNA).

(E) The rates of fork unwinding by 50 nM Hrq1 and hRecQ4 were similar ($t_{1/2}$ = time necessary to unwind 50% of the DNA).

(F) Hrq1 and Hrq1-KA bind ssDNA by gel shifts. Hrq1 also preferentially bound ss- versus dsDNA, as well as telomeric repeat ssDNA (TG₁₋₃).

(G) Directionality of Pif1 (lane 1), hRecQ4 (lane 2), and Hrq1 (lane 3) unwinding. The fastest migrating band corresponds to 5'-3' unwinding; the slower migrating band indicates 3'-5' activity.

(H) Sypro-orange-stained native gradient PAGE gel of Hrq1.

(I) TEM image of negative-stained Hrq1; white bar = 200 Å.

(J) Two-dimensional reconstruction of the Hrq1 heptamer. The inner and outer diameters of the ring are shown. All gel images are representative of three or more independent experiments, plotted data represent the average of three or more independent experiments, and error bars correspond to the SD.

See also [Figures S1](#) and [S5](#).

inactive Hrq1-KA, were purified from *E. coli* (Figure 1B; data not shown). In Hrq1-KA, the invariant lysine (K318) in the Walker A box was mutated to alanine (hereafter called KA alleles). The identity of the purified proteins was verified by western blotting and mass spectrometry (data not shown). Two earlier studies on fungal Hrq1 found that the *S. pombe* Hrq1 has minimal unwinding activity (Grocock et al., 2012), whereas *S. cerevisiae* Hrq1 requires a long (≥ 70 nt) 3' tail for activity (Kwon et al., 2012). In contrast, our recombinant *S. cerevisiae* Hrq1 displayed robust helicase activity, similar to that of hRecQ4 (Suzuki et al., 2009) (Figures 1C–1E and 1G), on a fork substrate with 25-nt single-stranded DNA (ssDNA) tails. Hrq1-KA had no activity (Figure 1C; data not shown), but it did bind ssDNA almost as well

as wild-type (WT) Hrq1 (Figure 1F). We also tested the ability of WT Hrq1 to bind double-stranded DNA (dsDNA) and a ssDNA substrate comprised of the *S. cerevisiae* telomeric repeat sequence TG₁₋₃. Hrq1 did not bind dsDNA (Figure 1F) but did bind TG₁₋₃ with weaker affinity ($K_d = 48 \pm 2$ nM) than for a poly(dT) substrate ($K_d = 800 \pm 69$ pM) but stronger than that for a poly(dG) or random sequence substrate (apparent $K_d = 260 \pm 60$ and 560 ± 20 nM, respectively; Figure 1F; data not shown).

All tested RecQ family helicases unwind DNA in the 3'-5' direction. Using a universal directionality substrate (Shin and Kelman, 2006), hRecQ4 and Hrq1 produced only the expected 3'-5' unwinding product, whereas purified *S. cerevisiae* Pif1 (a 5'-3' DNA helicase) yielded only the 5'-3' unwinding product

Table 1. Relative Sensitivity to DNA Damaging Agents

Genotype	DNA Damaging Agent								
	None ^a	Bleo	CPT	cisplatin	4NQO	HU	MMC	MMS	UV
WT	+++++	+++++	+++++	+++++	+++++	+++++	+++++	+++++	+++++
<i>hrq1Δ</i>	+++++	+++++	+++++	++++	++++	+++++	++	++++	+++++
<i>hrq1-KA</i>	+++++	+++++	+++++	++++	+++	+++++	+	++++	+++++
<i>sgs1Δ</i>	+++++	++++	+++	+	+	++	+++	+/-	+++
<i>sgs1-KA</i>	+++++	++++	+++	+	+	++	++++	+/-	+++
<i>hrq1Δ sgs1Δ</i>	+++++	+++++	+++	+	+/-	++	+	+/-	+++
<i>hrq1Δ sgs1-KA</i>	+++++	+++++	+++++	++++	+	Res	++	++++	+++++
<i>hrq1-KA sgs1Δ</i>	++++	+++	++	+	+/-	++	+/-	+/-	++
<i>hrq1-KA sgs1-KA</i>	+++++	+++++	+++	+	+/-	++	+/-	+/-	++++

The plates were incubated for 2 (YEPD, Bleo, CPT, 4NQO, and UV), 3 (cisplatin, MMC, and MMS), or 4 (HU) days at 30°C in the dark, and sensitivity was scored relative to growth of the WT strain on each plate. +++++, no sensitivity to the DNA damaging agent; +++++, no or poor growth of the 10⁻⁴ dilution (i.e., 10-fold sensitivity relative to WT); +++, 100-fold sensitivity, etc; +/-, little to no growth of the OD660 = 1 spot; Res, resistance to the drug relative to WT. ^aCells were diluted and plated as in Figure 2A on YEPD with (UV) or without (None) exposure to 100 J/m² ultraviolet radiation or on YEPD containing 5 μg/ml bleomycin (Bleo), 5 μg/ml camptothecin (CPT), 250 μg/ml cisplatin, 125 ng/ml 4-nitroquinoline-n-oxide (4NQO), 100 mM HU, 100 μg/ml MMC, or 0.03% methyl methanesulfonate (MMS).

(Figure 1G). Thus, like other known RecQs, *S. cerevisiae* Hrq1 is a 3'-5' DNA helicase and unwinds DNA with similar efficiency as hRecQ4.

To assess the oligomeric state of Hrq1, we subjected the purified protein to gel filtration and native gradient PAGE analysis. Gel filtration indicated that Hrq1 exists as a high molecular weight oligomer in solution (Figure S1). In native gradient PAGE, Hrq1 migrated as two prominent bands (Figure 1H) with apparent molecular weights >669 kDa (67% of the protein) and >200 kDa (33%). Negative staining and transmission electron microscopy (TEM) analysis demonstrated a prominent toroidal organization for Hrq1 (Figure 1I), and two-dimensional image averaging revealed that the particles are heptameric rings (Figure 1J).

Deletion of *HRQ1* Sensitizes Cells to ICLs

Mutation of disease-linked helicases often sensitizes cells to DNA damage. For instance, deletion of the *BLM* homolog *SGS1* renders *S. cerevisiae* sensitive to a wide range of genotoxic agents (see <http://www.yeastgenome.org/cgi-bin/locus.fpl?locus=sgs1> for a complete list). To compare the effects of loss of *HRQ1* to loss of *SGS1*, we deleted each gene and plated serial dilutions of cultures on rich media with or without DNA damaging agents. Catalytic inactivation of a helicase can be more detrimental than deletion of the gene encoding it if the inactive protein binds its sites of action and prevents a compensating activity from accessing those sites (Wu and Brosh, 2010). Therefore, we also tested inactive KA alleles of each gene, which were expressed from their native loci and produced stable protein in vivo (Figure S2). Finally, because hRecQ4 and hBLM interact in vivo (Singh et al., 2012), we also examined the effects of double *HRQ1/SGS1* mutants to determine if they have overlapping functions in DNA repair (Table 1; Figures 2A and 2B).

On rich media, there was no apparent growth difference in *hrq1Δ*, *hrq1-KA*, *sgs1Δ*, or *sgs1-KA* relative to WT (Figure 2A), though there were initial lags in the growth of some strains in liquid culture (Figure S3). We recapitulated the published *sgs1Δ* sensitivity to eight of eight agents (Table 1; Figures 2A

and 2B) and showed that *sgs1-KA* cells had similar patterns of sensitivity. With one exception, mutation of *HRQ1* had much milder effects than mutating *SGS1*; *hrq1Δ* and *hrq1-KA* cells had either WT or modestly reduced growth on seven agents to which *sgs1* cells showed strong sensitivity (bleomycin, camptothecin [CPT], cisplatin, 4-nitroquinoline-n-oxide [4NQO], hydroxyurea [HU], methyl methanesulfonate [MMS], and UV; see also Choi et al., 2013).

However, *hrq1Δ* and *hrq1-KA* cells were highly sensitive to MMC, a DNA crosslinker that generates mostly (~80%) inter-strand dG-dG crosslinks (Tomasz, 1995). Thus, Hrq1 acts catalytically during ICL repair. To determine if this sensitivity was specific to dG-dG ICLs, we tested the sensitivity of *hrq1* cells to 8-methoxypsoralen (8-MOP), which damages DNA only by inducing ICLs (usually dT-dT) after UV exposure (Averbeck and Averbeck, 1998). Both *hrq1Δ* and *hrq1-KA* cells were more sensitive to 8-MOP+UV treatment than WT (Figure 2C), again indicating that Hrq1 acts catalytically to promote ICL repair. However, *hrq1-KA* cells were much more sensitive than *hrq1Δ* (similar to the *rad52-1* control) (Henriques and Moustacchi, 1981), suggesting that Hrq1-KA binding to its ICL repair substrate blocks an alternative ICL repair pathway. *sgs1Δ* cells were not tested on 8-MOP+UV because they are sensitive to UV alone. Although *sgs1Δ* and *sgs1-KA* cells were only mildly MMC sensitive (Table 1; Figure 2A), *hrq1Δ sgs1Δ* cells were dead on MMC. Thus, Hrq1 has a more important role than Sgs1 in suppressing ICL damage, though Sgs1 may have a backup function in cells lacking Hrq1.

Previously, *PSO2*, which encodes a nuclease (Brendel et al., 2003), was the only *S. cerevisiae* gene known to suppress ICL damage specifically. We asked if Hrq1 and Pso2 act in the same ICL repair pathway by comparing the MMC sensitivity of WT, *hrq1Δ*, *pso2Δ*, and *hrq1Δ pso2Δ* strains. Although *pso2Δ* cells were ~10-fold more sensitive than *hrq1Δ* cells, the *hrq1Δ pso2Δ* double mutant displayed the same MMC sensitivity as *pso2Δ* over a range of MMC concentrations (Figure 2D). Thus, *hrq1Δ* is epistatic to *pso2Δ*, suggesting that Hrq1 and Pso2 act in the same ICL repair pathway.

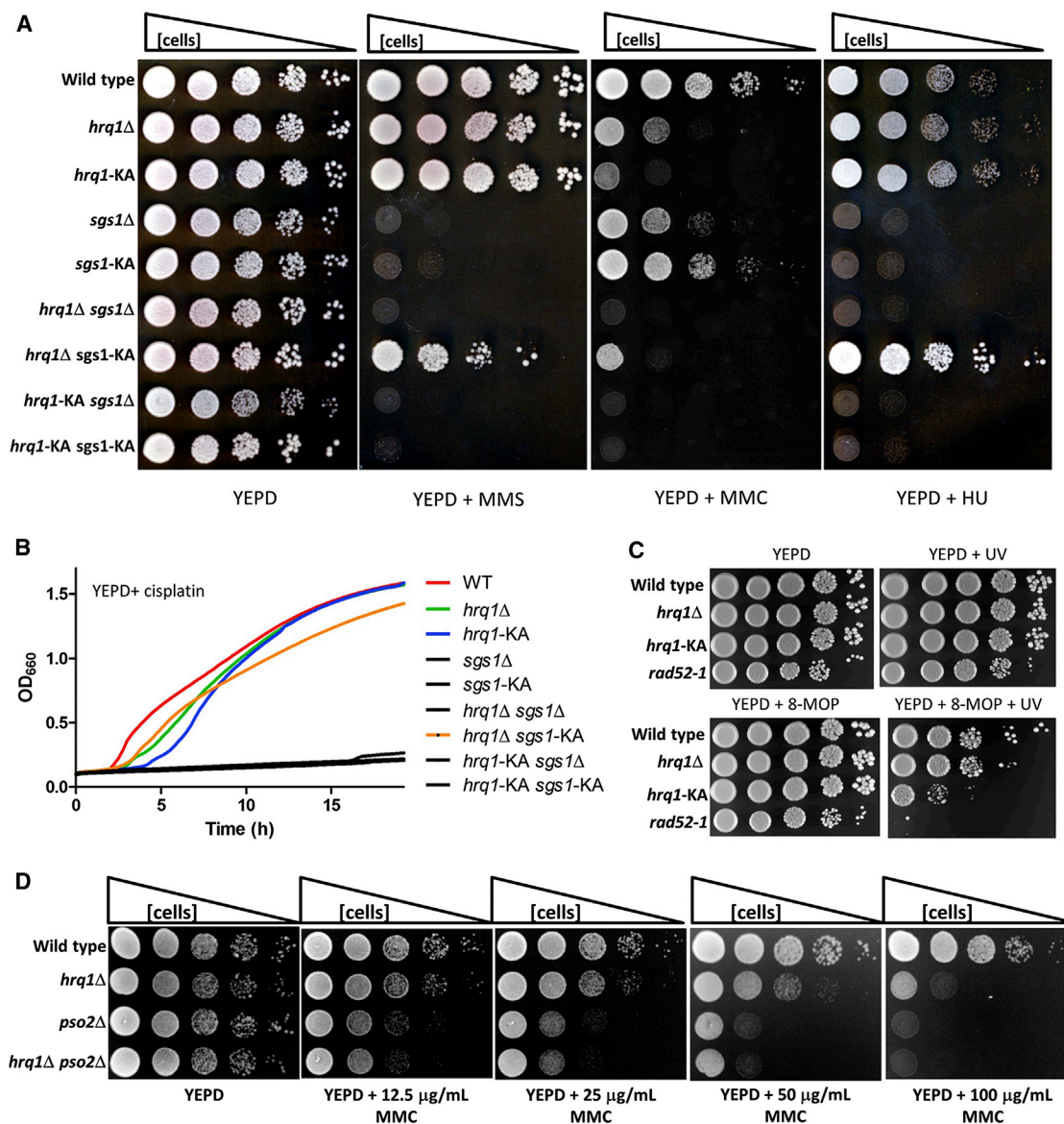


Figure 2. Comparison of *hrq1* and *sgs1* DNA Damage Sensitivity

(A) Growth of the indicated strains on YEPD and YEPD containing 0.03% MMS, 100 μ g/ml MMC, or 100 mM HU. Cells of the indicated genotype were grown in liquid culture, diluted to OD₆₆₀ = 1, and 10-fold serial dilutions were spotted onto plates, which were then incubated for 2 (YEPD), 3 (MMS and MMC), or 4 (HU) days in the dark.

(B) Growth curves of the indicated strains displaying relative sensitivity to cisplatin. Cells were grown overnight in YEPD, diluted to OD₆₆₀ = 0.1 in a 96-well plate, and incubated at 30°C in a BioTek EON plate reader with shaking. The OD₆₆₀ was then measured every 15 min for 24 hr. The plotted values are the means of three or more independent experiments per strain.

(C) 8-MOP+UV sensitivity of the indicated strains. Cells were grown, diluted, and spotted (as in A on YEPD plates or YEPD plates containing 20 μ M 8-MOP and either placed in an opaque container (YEPD and YEPD+8-MOP) or exposed to 365 nm UV for 5 (YEPD+8-MOP+UV) or 15 min (YEPD+UV) and then incubated in the dark for 2 days. The images are representative of results from triplicate experiments.

(D) *hrq1* Δ and *pso2* Δ are epistatic for MMC sensitivity. Cells were grown, diluted, and spotted (as in A on YEPD or YEPD+MMC plates and incubated for 2 days. See also Figures S2 and S3.

A reverse pattern of sensitivities was seen for cisplatin, which induces mostly (90%) 1,2-intrastrand crosslinks (Table 1; Figure 2B). More rarely, cisplatin generates dG-dG ICLs (Brabec, 2002). As reported, *sgs1* Δ cells were highly cisplatin sensitive (Liao et al., 2007), as were *sgs1*-KA cells. In contrast, *hrq1* and

hrq1-KA cells had only modest cisplatin sensitivity (see also Choi et al., 2013; Dittmar et al., 2013). Remarkably, deletion of *HRQ1* in the *sgs1*-KA strain strongly suppressed the *sgs1*-KA cisplatin sensitivity (Figure 2B). This suppression was not seen for other *hrq1* *sgs1* combinations, and its mechanism is unknown.

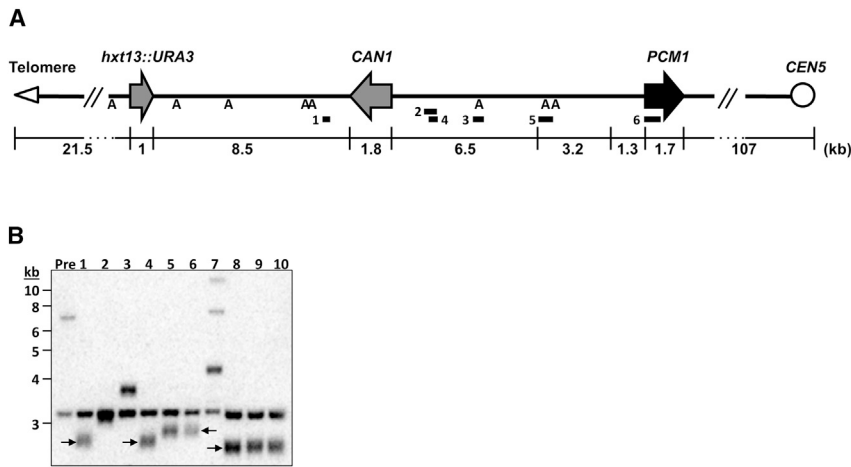


Figure 3. Deletion of *HRQ1* Affects De Novo Telomere Addition at DSBs

(A) Schematic of Chr V-L in the GCR strain. The numbered bars indicate the positions of the multiplex PCR products used to determine the relative locations of the GCR events. “A” denotes AlwNI restriction sites. *URA3* and *CAN1*, counterselectable markers; *PCM1*, first essential gene to the right of the V-L telomere.

(B) Southern blot analysis of representative *hrq1*Δ GCR clones. The blot was probed with the *CIN8* PCR product (primer pair 3 from A). TAs are denoted with arrows.

In general, deletion and KA alleles had similar effects on DNA damage sensitivity (Table 1). However, *hrq1*Δ *sgs1*-KA cells were more HU resistant than WT cells (Figure 2A). Although we did not explore the reason for these differences, they may reflect the dual roles of Sgs1 in activating the intra-S phase checkpoint, only one of which is helicase dependent (Frei and Gasser, 2000).

Deleting *HRQ1* Inhibits De Novo TA

In addition to drug sensitivities, helicase mutations often result in high rates of spontaneous DNA damage, such as gross-chromosomal rearrangements (GCRs), which are common in many cancers (Bernstein et al., 2010). The *S. cerevisiae* GCR assay provides a quantitative measure of such events by selecting for the simultaneous loss of expression of two counterselectable markers on the left arm of chromosome V (Chr V-L): *URA3* and *CAN1* (Figure 3A). Mutation of most yeast genes that are homologs of human tumor suppressor genes (e.g., *SGS1*) results in increased GCR rates (Myung et al., 2001b).

The *sgs1*Δ GCR rate was 16-fold higher than in WT cells ($p = 0.025$), similar to the ~20-fold increase reported previously (Myung et al., 2001b). The *sgs1*-KA strain had the same high GCR rate as *sgs1*Δ ($p = 0.020$), suggesting that the number of DNA lesions in the two strains was similar (Table 2). In contrast, the GCR rates in both *hrq1*Δ and *hrq1*-KA cells were only modestly higher than WT ($p = 0.043$ and 0.048 , respectively) (Table 2). The low GCR rate in *hrq1* mutants is consistent with our finding that these strains were insensitive to most types of DNA damage except ICLs (Table 1; Figure 3), which are rare for cells grown in laboratory conditions (Schärer, 2005). Indeed, pregrowth of *hrq1*Δ cells in media containing MMC prior to plating resulted in an ~58-fold increase in the GCR rate relative to cells treated with solvent alone (Table 2; data not shown). The GCR rate of WT cells grown under the same conditions also increased but only 5-fold.

If breaks occur between *CAN1* and *PCM1* (the most distal essential gene on Chr V-L; Figure 3A), FOA^R Can^R cells can theoretically be generated by TA to DSBs. However, in WT cells and virtually all single mutants, GCR events arise from recombination events that delete or move *URA3* and *CAN1* to new locations (Kolodner et al., 2002). The one published exception is *pif1* cells,

where most GCR events are due to TA (Myung et al., 2001a). To determine if GCR events were due to TA or recombination, we determined the structure of Chr V-L in multiple independent GCR clones from each mutant (Figures 3A and 3B; Table 2; data not shown).

As anticipated (Myung et al., 2001b), none of the WT (0/10) or *sgs1*Δ (0/15) GCR clones were due to TA, whereas 93% of the GCR events in *pif1*-*m2* (an allele that eliminates most of the nuclear Pif1 [Schulz and Zakian, 1994]) cells were TAs (52/56). Remarkably, ~80% (20/26) of the *hrq1*Δ GCR events were TAs (Table 2; Figure 3B). Also surprising, the events leading to the GCRs were different in *hrq1*-KA (4.5% TA, 1/22) and *hrq1*Δ (77% TAs) cells, even though the GCR rates were the same in these strains ($p = 0.264$). Thus, unlike Pif1, which requires helicase activity to inhibit telomerase (Myung et al., 2001a; Zhou et al., 2000), Hrq1 inhibited TA noncatalytically. In addition, *HRQ1* and *PIF1* did not act synergistically to suppress TAs, because the two helicases did not have additive effects on TA: the fraction of TAs in *hrq1*Δ *pif1*-*m2* cells was <50%, lower than in either single mutant. (See Discussion for a model explaining these data.)

We also determined the structure of Chr V-L in *sgs1*-KA GCR clones. Although TAs are not detected in *sgs1*Δ cells (Myung et al., 2001b) (Table 2), ~50% of the GCR events in *sgs1*-KA cells were TAs (11/24; Table 2). TAs are also detected in *sgs1*Δ *exo1*Δ cells, presumably because both pathways for DSB resection are blocked (Lydeard et al., 2010; Marrero and Symington, 2010). Because Sgs1-KA binds ssDNA (Cejka and Kowalczykowski, 2010), we suggest that it reduces Exo1 access (Figure 5A). Thus, both pathways to generate the ssDNA for strand invasion are inhibited, shifting the recombination-TA equilibrium toward TAs.

Hrq1 Limits Telomere Lengthening in *pif1*-*m2* Cells

The ability of Hrq1 to suppress TAs to DSBs suggested that, like Pif1, it might also inhibit telomerase lengthening of existing telomeres. However, telomere length was indistinguishable from WT in *hrq1*Δ and *hrq1*-KA cells (Figure 4A). In contrast, telomeres in *hrq1*Δ *pif1*-*m2* cells were even longer than in *pif1*-*m2*.

The hyperlengthening of telomeres in *hrq1*Δ *pif1*-*m2* cells could be due to recombination or telomerase. To distinguish between these possibilities, we analyzed telomere length in spore

Table 2. Gross-Chromosomal Rearrangement Rates and Analysis of Events in Independent Clones Grown in the Absence or Presence of Mitomycin C

Genotype	GCR Rate ^{a,b}	95% Confidence Interval	Telomere Addition (Clones Analyzed)
WT	1.0 ± 0.5 ^c	0.18–2.27	0% (10) ^c
WT + MMC	5 ± 4	2.52–11.5	ND
<i>sgs1</i> Δ	16 ± 5 ^c	5.15–37.4	0% (15) ^c
<i>sgs1</i> -KA	14 ± 3	13.1–40.1	46% ± 14% (24)
<i>hrq1</i> Δ	4 ± 2	3.19–12.6	77% ± 2.9% (26)
<i>hrq1</i> Δ + MMC	115 ± 30	89.6–188	ND
<i>hrq1</i> -KA	5 ± 3	3.48–16.7	4.5% ± 3.9% (22)
<i>hrq1</i> -KA + MMC	132 ± 42	46.5–246	ND
<i>pif1-m2</i>	76 ± 8 ^c	36.4–125	93% ± 7.6% (56) ^c

ND, not determined.

^aGross-chromosomal rearrangement (GCR) rates are the average of three or more independent experiments and are normalized to the WT rate ($1.5 \pm 0.7 \times 10^{-10}$ events/generation). ± denotes SD. + MMC denotes growth in media containing mitomycin C.

^bp values were calculated for the GCR rates for all pairwise combinations of strains. All mutant rates are significantly different from WT ($p = 0.025$, *sgs1*Δ; $p = 0.020$, *sgs1*-KA; $p = 0.043$, *hrq1*Δ; $p = 0.048$, *hrq1*-KA; and $p < 0.00005$, *pif1-m2*). All rates are significantly different from *pif1-m2* (all $p \leq 0.008$). The *hrq1*Δ and *hrq1*-KA GCR rates are not significantly different from either the *sgs1*Δ or *sgs1*-KA rates (all $p \geq 0.078$). For telomere additions, the frequency in *pif1-m2* cells was significantly different from all other strains (all $p < 0.030$), and the frequencies between *hrq1*Δ and *hrq1*-KA were also significantly different ($p = 0.0002$).

^cData are from Paeschke et al., 2013, though it was collected at the same time as the other data.

clones from a *pif1-m2*/WT *hrq1*Δ/WT *rad52*Δ/WT diploid (*Rad52* is a protein required for virtually all homologous recombination [HR] [Hiom, 1999]). Telomeres were even longer in *hrq1*Δ *pif1-m2* *rad52*Δ cells than in recombination-proficient cells (Figure 4A), demonstrating that the hyperlengthening was not recombination dependent. Telomeres are also longer in *rad52* versions of other mutants with long telomeres (e.g., *rif1* and *rif2*), suggesting that HR suppresses elongation in cells that already have long telomeres (Teng et al., 2000; Zhou et al., 2000). Thus, Hrq1 limits telomerase, not recombination, at *pif1-m2* telomeres.

Hrq1 did not act catalytically to inhibit telomerase at DSBs (Table 2). To determine if it acts catalytically to affect telomere length in *pif1-m2* cells, we analyzed telomeres in *hrq1*-KA *pif1-m2* and *hrq1*-KA *pif1-m2* *rad52*Δ cells. Telomere length was unaffected in the *hrq1*-KA *pif1-m2* background relative to *pif1-m2* (Figure 4A) (as expected, deletion of *RAD52* did increase *hrq1*-KA *pif1-m2* telomere length as seen for *pif1-m2* versus *rad52*Δ cells [Zhou et al., 2000]). Thus, Hrq1 acts structurally to inhibit lengthening of *pif1-m2* telomeres, just as it does during TA at DSBs.

Telomerase-Independent Telomere Maintenance by the Type I Pathway Is Hrq1 Dependent

In telomerase-deficient yeast and human cells, survivors arise that maintain telomeres by mechanisms that usually involve HR

(i.e., alternative lengthening of telomeres or ALT) (Wellinger and Zakian, 2012). In *S. cerevisiae*, telomerase-independent survivors come in two types: type I, which have tandem copies of the subtelomeric Y' element and very short tracts of telomeric DNA; and type II, which have heterogeneous length telomeres. Because hBLM (Stavropoulos et al., 2002) and Sgs1 (Huang et al., 2001; Johnson et al., 2001) both influence ALT, we asked if Hrq1 does as well. We sporulated an *hrq1*Δ/WT *sgs1*Δ/WT *tlc1*Δ/WT diploid strain (*TLC1* encodes telomerase RNA), serially restreaked spore clones until survivors appeared, and examined telomere structure in 20 survivors from each strain. As previously reported, *sgs1*Δ *tlc1*Δ spore clones generated only type I survivors. In contrast, all *hrq1*Δ *tlc1*Δ survivors had type II telomeres; *sgs1*Δ was epistatic to *hrq1*Δ because all *hrq1*Δ *sgs1*Δ *tlc1*Δ survivors were type I (Figure 4B). Thus, Hrq1 is required to generate type I survivors in the presence of Sgs1.

Hrq1 Binds Telomeres In Vivo

If Hrq1 affects telomeres directly, it will bind telomeres, which might be detectable by chromatin immunoprecipitation (ChIP). In WT cells, Hrq1-13xMyc bound significantly to telomere VI-R (relative to a control site; $p < 0.001$); binding to the VII-L telomere was detectable but not significant ($p = 0.0567$; Figure 4C). However, in *pif1-m2* cells, Hrq1 binding was significant at both ($p < 0.001$; ~2.5-fold higher to *pif1-m2* versus WT telomeres). These results suggest that Hrq1 is telomere associated in WT cells but that Pif1 can displace it from telomeres. This interpretation also explains why telomeres in *hrq1*Δ cells are of WT length (Figure 4A).

DISCUSSION

Hrq1 Protects against ICLs

Unlike *sgs1* cells, *hrq1* cells were resistant to most DNA damaging agents (Table 1). This pattern is reminiscent of the damage sensitivities for their human homologs, because hRecQ4-deficient cells are less sensitive than hBLM mutant cells to many DNA damaging agents, including cisplatin (see Mao et al., 2010 and references therein). However, a different pattern was seen for two ICL-inducing agents: *hrq1*Δ and *hrq1*-KA cells were highly sensitive to both MMC and 8-MOP. Thus, Hrq1 acts catalytically to promote ICL repair. Cells expressing Hrq1-KA were much more sensitive to these agents than *hrq1*Δ cells (Figures 2A and 2C). This finding suggests that Hrq1 is the main helicase in ICL repair, and its backup is hindered from accessing the DNA because Hrq1-KA is bound to sites of damage. The even higher MMC sensitivity of *hrq1* *sgs1* cells (Figure 2A) suggests that Sgs1 is the backup for Hrq1 at ICLs. Even the modest sensitivity of *hrq1* cells to cisplatin, a predominantly intrastrand cross-linker (Table 1; Figure 2B), can be explained by its role in ICL repair, because ~5% of cisplatin lesions are ICLs (Brabec, 2002).

Our study reports MMC and 8-MOP sensitivity for *hrq1* *S. cerevisiae*, but *S. pombe* *hrq1*Δ cells have previously been reported as highly sensitive to both cisplatin and MMC (Grocock et al., 2012). However, because 8-MOP was not tested in that study, it is possible that the *S. pombe* *hrq1*Δ MMC sensitivity is due to the low level of intrastrand crosslinks generated by MMC. In any case, because *S. cerevisiae* Sgs1 has quite different

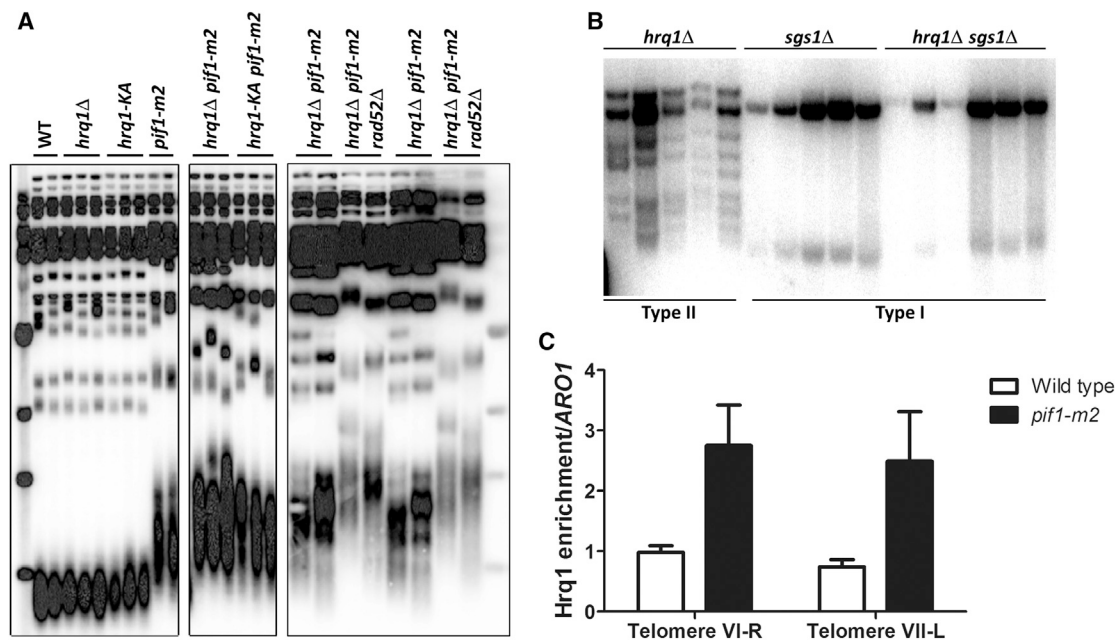


Figure 4. Hrq1 Affects Telomere Maintenance

(A) Telomere blots of gDNA from the indicated strains. Two leftmost panels are cropped from a gel with intervening lanes removed; see Figure S4.

(B) Telomere blot of gDNA from *tlc1Δ* survivors from the indicated strains after growth in the absence of *TLC1* and the indicated helicases.

(C) Increased Hrq1-Myc binding to telomeres. Binding was normalized to input DNA and *ARO1*. The data are the mean of five independent experiments, and the error bars correspond to the SD.

See also Figure S4.

in vivo functions from its *S. pombe* homolog Rqh1 (Ashton and Hickson, 2010; Cromie et al., 2008), it is not surprising that Hrq1 also functions differently in these distantly related yeasts.

ICLs are dangerous because covalent linkage of the two DNA strands prevents both transcription and DNA replication. In addition, ICLs are of medical interest as patients with Fanconi's anemia (FA), an inherited disease arising from mutation in any of 16 FA genes, are defective in their repair (Clouston et al., 2013). Recently, putative yeast homologs of some of the FA proteins have been identified, but single mutants in these genes are not sensitive to ICL agents (Daee et al., 2012; Daee and Myung, 2012; Ward et al., 2012). Whereas mammals have multiple helicases that suppress ICL damage (e.g., HELQ acts in a pathway parallel to FA to suppress ICL damage [Adelman et al., 2013]), our study identifies a helicase, Hrq1, whose elimination renders *S. cerevisiae* highly ICL sensitive. Indeed, *HRQ1* and *PSO2* are the only *S. cerevisiae* genes that specifically suppress ICL damage, and genetic data indicate that they act in the same pathway (Figure 2D). We do not know how Hrq1 acts to facilitate ICL repair, but one possibility is that it functions analogously to HEL308, a human 3'-5' helicase involved in crosslink repair (Moldovan et al., 2010). hRecQ4 is also implicated in ICL repair (Larizza et al., 2010), and Hrq1 may be its functional homolog in yeast ICL repair.

Hrq1 Affects Diverse Aspects of Telomere Biology

Our analysis revealed multiple telomere functions for Hrq1. Given that Hrq1 was present by ChIP at telomeres, especially in *pif1-m2* cells (Figure 4C), Hrq1 likely affects telomeres directly.

Hrq1 impacts the two major pathways of telomere maintenance: telomerase and recombination. It inhibited telomerase-mediated telomere lengthening in *pif1-m2* cells (Figure 4A) and promoted type I survivor formation in *tlc1Δ* cells (Figure 4B). Generation of type II survivors is Sgs1 dependent (Huang et al., 2001; Johnson et al., 2001) (Figure 4B). Thus, as with crosslink repair, the two *S. cerevisiae* RecQ helicases have complementary effects on telomerase-independent telomere maintenance.

The most unexpected telomere effect of Hrq1 is its noncatalytic inhibition of TA. Remarkably, 77% of the GCR events in *hrq1Δ* cells were TAs (Table 2). Until this report, *pif1* was the only single mutant in which TAs are easily detected (93% TA; Table 2) (Myung et al., 2001a; Paeschke et al., 2013). In vivo and in vitro, Pif1 uses its ATPase activity to remove telomerase from DNA ends, and, thus, TA increases in *pif1Δ*, *pif1-m2*, and *pif1-KA* cells (Boulé et al., 2005; Myung et al., 2001a; Zhou et al., 2000). If Hrq1 also removes telomerase, *hrq1-KA* cells should have high TA rates, and nearly all *hrq1Δ pif1-m2* GCR events should be TAs. In contrast, TAs were rare in *hrq1-KA* (4.5%) and considerably lower in *hrq1Δ pif1-m2* (46%) cells than in either single mutant. This structural role of Hrq1 is the key to understanding its mechanism of action at both DSBs and telomeres.

There are two major pathways for DSB repair in yeast: HR and TA. These pathways can be thought of as being in competition with each other, even though TA is rare in WT cells and virtually all tested mutants. Inhibiting TA is critical for genome integrity because it results in aneuploidy for all sequences distal to the TA.

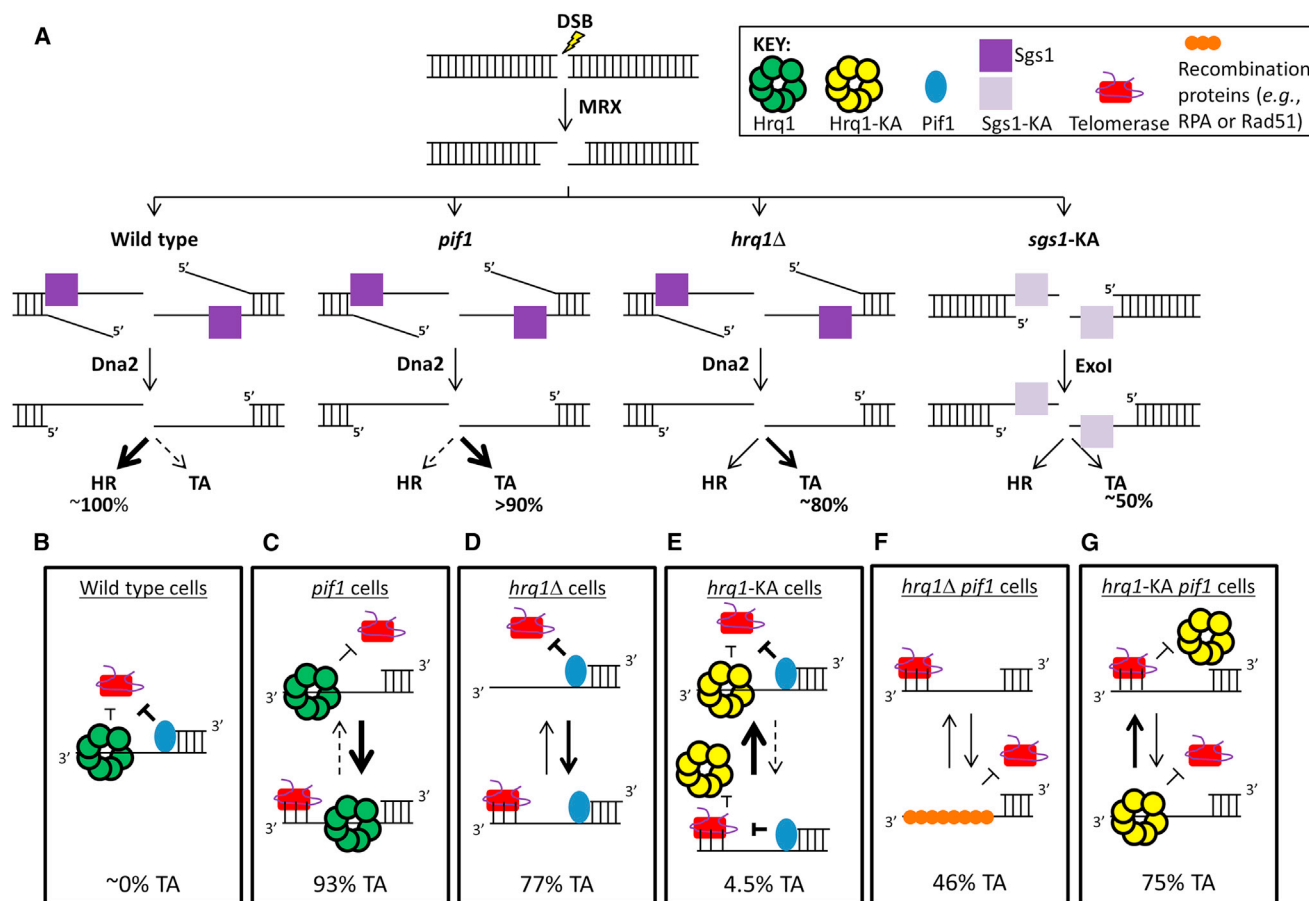


Figure 5. Model for Effects of Helicases on TA at DSBs

(A) DSB processing by 5' end resection in the presence (dark purple) and absence (light purple) of Sgs1 activity (Zhu et al., 2008). A DSB is initially processed by the MRX complex, and then 5' end resection occurs via the action of Sgs1 and the nuclease Dna2 in WT cells or Exo1 in *sgs1Δ* (not shown) and *sgs1-KA* cells. In WT cells, virtually all DSBs are healed by HR rather than TA. Three ways to shift this balance toward TA are to mutate *PIF1*, delete *HRQ1*, and express inactive Sgs1. (B–G) Likelihood of TA at a DSB in (B) WT, (C) *pif1*, (D) *hrq1Δ*, (E) *hrq1-KA*, (F) *hrq1Δ pif1*, and (G) *hrq1-KA pif1* cells. See Discussion for a detailed explanation. Note that Pif1 is shown bound to the ss/dsDNA junction because single-molecule analysis indicates that this is its preferred binding position, and it does not translocate from this position toward the 3' end of the recessed strand (R. Zhou, M.L.B., V.A.Z., and T. Ha, unpublished data).

See also Figures S1 and S5.

The balance between TA and recombination can be altered by preventing HR, as in *sgs1Δ exo1Δ* (Lydeard et al., 2010; Marrero and Symington, 2010) or *sgs1-KA* cells (Table 2) or by eliminating a telomerase inhibitor, as in *pif1* cells. Hrql is unlikely to affect the HR-TA balance by promoting recombination, because it has not been recovered in the large number of screens for genes that affect recombination. Its binding to telomeres (Figure 4C) and inhibition of telomerase at *pif1-m2* telomeres (Figure 4A) also argue that it affects telomerase, not recombination, at DSBs.

We propose a working model in which Hrql inhibits telomerase by competing with it for ssDNA binding (Figures 5D and 5E). According to this model, TA is frequent in *hrq1Δ* GCR clones because telomerase has better access to its substrate (but not as frequent as in *pif1-m2* cells because Pif1 is still there to remove telomerase; Figure 5D). TA is infrequent in *hrq1-KA* cells because inactive Hrql-KA still binds ssDNA (Figure 1F) and

competes with telomerase for ssDNA binding (Figure 5E). We propose that Hrql/Hrql-KA also compete with recombination proteins (e.g., RPA or Rad51) for binding to ssDNA. This hypothesis would explain why TA was not as frequent in *hrq1Δ pif1-m2* cells as in either single mutant because recombination proteins and telomerase then compete with each other for ssDNA in the absence of both Pif1 and Hrql (Figure 5F). Consistent with this model, Hrql bound preferentially to ss- versus dsDNA (Figure 1F).

The same model can explain how Hrql affects telomeres (Figure 4A). It predicts that Pif1 expels both telomerase and Hrql from telomeres, so *hrq1Δ* telomeres are WT in length. However, telomeres were longer in *hrq1Δ pif1-m2* than *pif1-m2* cells (Figures 4A, 4B, and 5A) because when Pif1 is absent, Hrql (or Hrql-KA) limits telomerase by competing with it for binding to telomeric ssDNA. Consistent with this hypothesis, Hrql bound single-stranded telomeric DNA in vitro (Figure 1F).

In summary, our studies show that Hrq1 has two roles that promote genome integrity: (1) It acts catalytically to promote ICL repair. Indeed, the very strong ICL sensitivity of *hrq1*-KA cells suggests that Hrq1 may be the first line of defense against these dangerous lesions. (2) We also found that Hrq1 affects several aspects of telomere biology, including inhibition of telomerase at DSBs and telomeres. Two of the defects in *hrq1* cells, sensitivity to ICLs and frequent TAs, are rare phenotypes; the demonstration of both functions in one protein is unprecedented. If hRecQ4 has either or both activities, this could explain why its mutation results in genomic instability and disease.

EXPERIMENTAL PROCEDURES

Yeast Strains, Media, and Other Reagents

All strains (Table S1) were created by standard methods and are derivatives of the YPH background (Sikorski and Hieter, 1989). Cells were grown in standard *S. cerevisiae* media at 30°C unless indicated. ³²P-dCTP and ³²P-ATP were purchased from PerkinElmer, and unlabeled ATP was from GE Healthcare. DNA damaging agents were from Sigma. All restriction enzymes were from NEB, and all oligonucleotides were from IDT.

Protein Purification

Details on *HRQ1* and *hrq1*-KA cloning and expression vector construction, as well as the complete protein purification protocol, can be found in the Supplemental Experimental Procedures. Briefly, expression plasmids were transformed into Rosetta 2(DE3) pLysS cells, and recombinant protein was expressed using the autoinduction method (Studier, 2005). Cells were harvested by centrifugation. The pellets were resuspended in buffer and lysed by adding *n*-dodecyl β-D-maltoside (DM; Sigma) to a final concentration of 0.05% (w/v) and 1 × FastBreak (Promega).

The soluble fraction was clarified by centrifugation and filtering through a 0.22 μm membrane. This mixture was then loaded onto a Strep-Tactin Sepharose column (IBA), and protein was eluted with three column volumes (CVs) of desthiobiotin buffer after extensive washing. Peak fractions were pooled and loaded onto a His60 Ni column (Clontech). After washing, protein was eluted with six CVs of imidazole buffer, and peak fractions were pooled and concentrated by ultrafiltration. The protein was then buffer-exchanged into storage buffer using a desalting column.

The hRecQ4 expression plasmid pGEX-RecQ4-His9 was a gift from Patrick Sung, Yale University. hRecQ4 was purified as described (Macris et al., 2006). The protein concentration and purity of the final preparations were determined on SYPRO orange-stained SDS-PAGE gels using known amounts of a standard protein for comparison. In all cases, protein purity was ≥95%.

Helicase Assays

The fork substrate was constructed by end labeling oligonucleotide MB733 (Table S2) with T4 PNK and γ³²P-ATP and separating the ssDNA from free label using a G-50 micro column (GE Healthcare). Labeled MB733 was then annealed to oligonucleotide MB734 in 1 × NEB buffer #2 by boiling and slowly cooling to room temperature. The directionality substrate was similarly constructed by end labeling an equimolar mixture of oligonucleotides MB453 and 454 (Table S2) and removing free label using a G-50 micro column. The labeled oligonucleotides were then annealed to MB452 as above. Both substrates were separated from contaminating ssDNA by gel purification, followed by electroelution into a dialysis membrane.

Helicase reactions were performed in 1 × binding buffer (25 mM Na-HEPES [pH 8.0], 5% glycerol, 50 mM NaOAc, 150 μM NaCl, 7.5 mM MgOAc, and 0.01% DM) and contained 0.1 nM radiolabeled substrate, protein as indicated, 5 mM ATP, and 15 nM unlabeled oligonucleotide MB733 (fork) or MB453 and MB454 (directionality). Hrq1 helicase activity was unaffected by omitting these unlabeled ssDNA traps (e.g., Figure S5). Reactions containing the directionality substrate additionally contained 100 μg/ml Neutravidin (Pierce). The reactions were incubated at 37°C for 30 min and stopped by the addition of 1 × stop-load buffer (25% [w/v] Ficoll (type 400), 100 mM EDTA, 0.1% SDS,

0.25% bromophenol blue, and 0.25% xylene cyanol). The samples were then separated on 8% 29:1 acrylamide:bis-acrylamide gels in 1 × TBE buffer at 100 V/cm for 30–45 min, dried, and imaged/quantified using a Typhoon 9410 scanner and Image Gauge software.

Native Gradient Gel Electrophoresis

Native gradient gels were poured following the protocol in the Supplemental Experimental Procedures. Protein (≥0.5 μg) was loaded into the wells in the absence of loading dye and run at 17 V/cm for 3–6 hr in 20 mM Tris-HCl (pH 8.8) and 200 mM glycine. After electrophoresis, gels were incubated in 0.05% SDS for 15 min, rinsed with water, and stained with SYPRO orange overnight prior to analysis as described above for protein concentration.

TEM

Hrq1 was analyzed by TEM essentially as previously described for the Mcm2-7 helicase (Bochman and Schwacha, 2007). Briefly, the protein was diluted to 25 μg/ml in storage buffer, absorbed to glow-discharged copper grids (Ted Pella), and negatively stained with 2% uranyl acetate. Grids were visualized with a LEO OMEGA 912 electron microscope (Carl Zeiss) at 80 kV and 40,000 × magnification. Micrographs were taken with a 7.5 megapixel EMCCD camera (Peltier-cooled Hamamatsu ORCA) and visualized with AMT (v.602) software. Two-dimensional image averaging of Hrq1 complexes was performed using EMAN2 (Tang et al., 2007).

GCR Assays

GCR assays were performed essentially as described by Putnam and Kolodner (2010). Briefly, three or more sets of five or more 5 ml cultures of each *S. cerevisiae* GCR strain (Table 1) were grown to saturation in YEPD medium ± 25 μg/ml MMC at 30°C for 36–48 hr. Cells (2 ml) from each culture were pelleted, resuspended in sterile water, plated on dropout medium lacking uracil and arginine (US Biologicals) supplemented with 1 g/l 5-FOA and 60 mg/l canavanine sulfate (FOA+Can), and incubated at 30°C for 4 days. GCR rates (per 10⁻⁹ mutations/generation) and 95% confidence intervals were calculated using the FALCOR web server and MMS Maximum Likelihood Method (Hall et al., 2009). The rates presented are the means ± SDs of three or more experiments per strain. *p* values were calculated using Student's *t* test. We define GCR clones as colonies that grew on the FOA+Can plates. Such FOA^R Can^R clones were selected for post-GCR analyses (multiplex PCR [Supplemental Experimental Procedures] and Southern blotting, below).

Southern Blotting

When colonies arose after GCR events, they were restreaked onto FOA+Can plates to verify the FOA^R Can^R phenotype and grown overnight in YEPD liquid media at 30°C, and genomic DNA (gDNA) was isolated. The gDNA was analyzed by multiplex PCR and Southern blotting as described (Paeschke et al., 2013). Briefly, gDNA from clones retaining the *CIN8* PCR product was digested overnight at 37°C with AlwNI, run on 0.7% agarose gels, and blotted on Hybond-XL membranes (GE Life Sciences). For the Southern blots, the 400 bp *CIN8* PCR product was used a probe (hybridization sites are shown in Figure 3A), resulting in a 3.2 kb background band in all lanes. A non-GCR event yields a 6.9 kb band, TAs produce fuzzy bands <5 kb, and non-TAs result in sharp bands.

For telomere blots, gDNA was isolated from cells as described above. For the experiments examining the effect of recombination on telomere length, heterozygous diploids (Table S1) were sporulated, tetrads were dissected, and three spore clones of the desired genotypes were serially restreaked on YEPD for ~100 generations prior to gDNA isolation. For standard telomere length detection, gDNA was digested overnight with PstI and XhoI, whereas for telomere blots from *tlc1Δ* survivors, the gDNA was digested overnight with XhoI. Digests were separated on 1% agarose gels and transferred as described above. In both types of telomere blots, the probe used was a previously described C₁₋₃ATG₁₋₃ restriction fragment (Runge and Zakian, 1989).

tlc1Δ Survivor Analysis

The generation and analysis of telomeric survivors were performed as described previously (Teng and Zakian, 1999). Briefly, a *HRQ1/hrq1Δ* *SGS1/sgs1Δ* *TLC1/tlc1Δ* diploid strain (KP386) was generated, sporulated, and

hrq1Δ tlc1Δ and *sgs1Δ tlc1Δ* spores were identified by plating. Spores were restreaked four to five times (~25 generations/streak) on YC plates until survivors formed. For each spore clone, ten colonies were picked for the next restreak. In total, gDNA was isolated from 20 different spores for each strain background and analyzed as described above.

Chromatin Immunoprecipitation

Chromatin immunoprecipitation (ChIP) of asynchronous yeast cells growing in YEPD was performed as described (Azvolinsky et al., 2009) and analyzed using an iCycleriQ Real-Time PCR detection system (Bio-Rad). *Hrq1* was C-terminally tagged with 13 Myc epitopes, and ChIP was performed using a Myc monoclonal antibody (Clontech #631206). The amount of DNA in the immunoprecipitate was normalized to the amount in input samples. The ChIP experiment was analyzed by quantitative PCR (qPCR) in duplicate or triplicate to obtain an average value for each sample. The ChIP experiment was repeated three times at each locus. For each qPCR experiment, the amount of signal in the *Hrq1* immunoprecipitate was normalized to input and to the immunoprecipitated signal from *ARO1*.

SUPPLEMENTAL INFORMATION

Supplemental Information includes Supplemental Experimental Procedures, five figures, and two tables and can be found with this article online at <http://dx.doi.org/10.1016/j.celrep.2013.12.037>.

ACKNOWLEDGMENTS

M.L.B. dedicates this article to the memory of Megan Davey who passed away during the course of this work. We thank Kathy Friedman, Margaret Platts, Kristina Schmidt, Raymund Wellinger, and Nadine Guenther for sharing their methods, suggesting experiments, for useful discussions, and assistance with experiments. Research in the Zakian laboratory is supported by grants from the National Institutes of Health (GM26938 and GM GM43265) and postdoctoral fellowships from the American Cancer Society (to M.L.B.; PF-10-145-01-DMC), the Deutsche Forschungsgemeinschaft (to K.P.), and the New Jersey Commission on Cancer Research (to K.P.). Research in the Paeschke laboratory is supported by the Emmy-Noether Program of the Deutsche Forschungsgemeinschaft.

Received: October 14, 2013

Revised: November 27, 2013

Accepted: December 24, 2013

Published: January 16, 2014

REFERENCES

- Abdelhaleem, M. (2010). Helicases: an overview. *Methods Mol. Biol.* 587, 1–12.
- Adelman, C.A., Lolo, R.L., Birkbak, N.J., Murina, O., Matsuzaki, K., Horejsi, Z., Parmar, K., Borel, V., Skehel, J.M., Stamp, G., et al. (2013). HELQ promotes RAD51 paralogue-dependent repair to avert germ cell loss and tumorigenesis. *Nature* 502, 381–384.
- Ashton, T.M., and Hickson, I.D. (2010). Yeast as a model system to study RecQ helicase function. *DNA Repair (Amst.)* 9, 303–314.
- Averbeck, D., and Averbeck, S. (1998). DNA photodamage, repair, gene induction and genotoxicity following exposures to 254 nm UV and 8-methoxypsoralen plus UVA in a eukaryotic cell system. *Photochem. Photobiol.* 68, 289–295.
- Azvolinsky, A., Giresi, P.G., Lieb, J.D., and Zakian, V.A. (2009). Highly transcribed RNA polymerase II genes are impediments to replication fork progression in *Saccharomyces cerevisiae*. *Mol. Cell* 34, 722–734.
- Barea, F., Tessaro, S., and Bonatto, D. (2008). In silico analyses of a new group of fungal and plant RecQ4-homologous proteins. *Comput. Biol. Chem.* 32, 349–358.
- Bernstein, K.A., Gangloff, S., and Rothstein, R. (2010). The RecQ DNA helicases in DNA repair. *Annu. Rev. Genet.* 44, 393–417.
- Bochman, M.L., and Schwacha, A. (2007). Differences in the single-stranded DNA binding activities of MCM2-7 and MCM467: MCM2 and MCM5 define a slow ATP-dependent step. *J. Biol. Chem.* 282, 33795–33804.
- Boulé, J.B., Vega, L.R., and Zakian, V.A. (2005). The yeast Pif1p helicase removes telomerase from telomeric DNA. *Nature* 438, 57–61.
- Brabec, V. (2002). DNA modifications by antitumor platinum and ruthenium compounds: their recognition and repair. *Prog. Nucleic Acid Res. Mol. Biol.* 71, 1–68.
- Brendel, M., Bonatto, D., Strauss, M., Revers, L.F., Pungartnik, C., Saffi, J., and Henriques, J.A. (2003). Role of PSO genes in repair of DNA damage of *Saccharomyces cerevisiae*. *Mutat. Res.* 544, 179–193.
- Capp, C., Wu, J., and Hsieh, T.S. (2010). RecQ4: the second replicative helicase? *Crit. Rev. Biochem. Mol. Biol.* 45, 233–242.
- Cejka, P., and Kowalczykowski, S.C. (2010). The full-length *Saccharomyces cerevisiae* Sgs1 protein is a vigorous DNA helicase that preferentially unwinds Holliday junctions. *J. Biol. Chem.* 285, 8290–8301.
- Chisholm, K.M., Aubert, S.D., Freese, K.P., Zakian, V.A., King, M.C., and Welch, P.L. (2012). A genome-wide screen for suppressors of Alu-mediated rearrangements reveals a role for PIF1. *PLoS ONE* 7, e30748.
- Choi, D.H., Lee, R., Kwon, S.H., and Bae, S.H. (2013). *Hrq1* functions independently of *Sgs1* to preserve genome integrity in *Saccharomyces cerevisiae*. *J. Microbiol.* 51, 105–112.
- Clauson, C., Scharer, O.D., and Niedernhofer, L. (2013). Advances in understanding the complex mechanisms of DNA interstrand cross-link repair. *Cold Spring Harbor perspectives in medicine* 3, a012732.
- Cromie, G.A., Hyppa, R.W., and Smith, G.R. (2008). The fission yeast BLM homolog Rqh1 promotes meiotic recombination. *Genetics* 179, 1157–1167.
- Dae, D.L., Ferrari, E., Longerich, S., Zheng, X.F., Xue, X., Branzei, D., Sung, P., and Myung, K. (2012). Rad5-dependent DNA repair functions of the *Saccharomyces cerevisiae* FANCM protein homolog Mph1. *J. Biol. Chem.* 287, 26563–26575.
- Dae, D.L., and Myung, K. (2012). Fanconi-like crosslink repair in yeast. *Genome integrity* 3, 7.
- Dittmar, J.C., Pierce, S., Rothstein, R., and Reid, R.J. (2013). Physical and genetic-interaction density reveals functional organization and informs significance cutoffs in genome-wide screens. *Proc. Natl. Acad. Sci. USA* 110, 7389–7394.
- Frei, C., and Gasser, S.M. (2000). The yeast Sgs1p helicase acts upstream of Rad53p in the DNA replication checkpoint and colocalizes with Rad53p in S-phase-specific foci. *Genes Dev.* 14, 81–96.
- Grocock, L.M., Prudden, J., Perry, J.J., and Boddy, M.N. (2012). The RecQ4 orthologue *Hrq1* is critical for DNA interstrand cross-link repair and genome stability in fission yeast. *Mol. Cell. Biol.* 32, 276–287.
- Hall, B.M., Ma, C.X., Liang, P., and Singh, K.K. (2009). Fluctuation analysis CalculatOR: a web tool for the determination of mutation rate using Luria-Delbruck fluctuation analysis. *Bioinformatics* 25, 1564–1565.
- Henriques, J.A., and Moustacchi, E. (1981). Interactions between mutations for sensitivity to psoralen photoaddition (psd) and to radiation (rad) in *Saccharomyces cerevisiae*. *J. Bacteriol.* 148, 248–256.
- Hiom, K. (1999). Dna repair: Rad52 - the means to an end. *Curr. Biol.* 9, R446–R448.
- Huang, P., Pryde, F.E., Lester, D., Maddison, R.L., Borts, R.H., Hickson, I.D., and Louis, E.J. (2001). SGS1 is required for telomere elongation in the absence of telomerase. *Curr. Biol.* 11, 125–129.
- Jin, W., Liu, H., Zhang, Y., Otta, S.K., Plon, S.E., and Wang, L.L. (2008). Sensitivity of RECQL4-deficient fibroblasts from Rothmund-Thomson syndrome patients to genotoxic agents. *Hum. Genet.* 123, 643–653.
- Johnston, F.B., Marciniak, R.A., McVey, M., Stewart, S.A., Hahn, W.C., and Guarente, L. (2001). The *Saccharomyces cerevisiae* WRN homolog Sgs1p participates in telomere maintenance in cells lacking telomerase. *EMBO J.* 20, 905–913.

- Kolodner, R.D., Putnam, C.D., and Myung, K. (2002). Maintenance of genome stability in *Saccharomyces cerevisiae*. *Science* 297, 552–557.
- Kwon, S.H., Choi, D.H., Lee, R., and Bae, S.H. (2012). *Saccharomyces cerevisiae* Hrq1 requires a long 3'-tailed DNA substrate for helicase activity. *Biochem. Biophys. Res. Commun.* 427, 623–628.
- Larizza, L., Roversi, G., and Volpi, L. (2010). Rothmund-Thomson syndrome. *Orphanet J. Rare Dis.* 5, 2.
- Lee, W., St Onge, R.P., Proctor, M., Flaherty, P., Jordan, M.I., Arkin, A.P., Davis, R.W., Nislow, C., and Giaever, G. (2005). Genome-wide requirements for resistance to functionally distinct DNA-damaging agents. *PLoS Genet.* 1, e24.
- Liao, C., Hu, B., Arno, M.J., and Panaretou, B. (2007). Genomic screening in vivo reveals the role played by vacuolar H⁺ ATPase and cytosolic acidification in sensitivity to DNA-damaging agents such as cisplatin. *Mol. Pharmacol.* 71, 416–425.
- Liu, Y. (2010). Rothmund-Thomson syndrome helicase, RECQ4: on the crossroad between DNA replication and repair. *DNA Repair (Amst.)* 9, 325–330.
- Lydeard, J.R., Lipkin-Moore, Z., Jain, S., Eapen, V.V., and Haber, J.E. (2010). Sgs1 and exo1 redundantly inhibit break-induced replication and de novo telomere addition at broken chromosome ends. *PLoS Genet.* 6, e1000973.
- Macris, M.A., Krejci, L., Bussen, W., Shimamoto, A., and Sung, P. (2006). Biochemical characterization of the RECQ4 protein, mutated in Rothmund-Thomson syndrome. *DNA Repair (Amst.)* 5, 172–180.
- Mao, F.J., Sidorova, J.M., Lauper, J.M., Emond, M.J., and Monnat, R.J. (2010). The human WRN and BLM RecQ helicases differentially regulate cell proliferation and survival after chemotherapeutic DNA damage. *Cancer Res.* 70, 6548–6555.
- Marrero, V.A., and Symington, L.S. (2010). Extensive DNA end processing by exo1 and sgs1 inhibits break-induced replication. *PLoS Genet.* 6, e1001007.
- Mirzaei, H., Syed, S., Kennedy, J., and Schmidt, K.H. (2011). Sgs1 truncations induce genome rearrangements but suppress detrimental effects of BLM overexpression in *Saccharomyces cerevisiae*. *J. Mol. Biol.* 405, 877–891.
- Moldovan, G.L., Madhavan, M.V., Mirchandani, K.D., McCaffrey, R.M., Vinciguerra, P., and D'Andrea, A.D. (2010). DNA polymerase POLN participates in cross-link repair and homologous recombination. *Mol. Cell. Biol.* 30, 1088–1096.
- Myung, K., Chen, C., and Kolodner, R.D. (2001a). Multiple pathways cooperate in the suppression of genome instability in *Saccharomyces cerevisiae*. *Nature* 411, 1073–1076.
- Myung, K., Datta, A., Chen, C., and Kolodner, R.D. (2001b). SGS1, the *Saccharomyces cerevisiae* homologue of BLM and WRN, suppresses genome instability and homologous recombination. *Nat. Genet.* 27, 113–116.
- Paeschke, K., Bochman, M.L., Garcia, P.D., Cejka, P., Friedman, K.L., Kowalczykowski, S.C., and Zakian, V.A. (2013). Pif1 family helicases suppress genome instability at G-quadruplex motifs. *Nature* 497, 458–462.
- Putnam, C.D., and Kolodner, R.D. (2010). Determination of gross chromosomal rearrangement rates. *Cold Spring Harb. Protoc.* Published online September 1, 2010. <http://dx.doi.org/10.1101/pdb.prot5492>.
- Runge, K.W., and Zakian, V.A. (1989). Introduction of extra telomeric DNA sequences into *Saccharomyces cerevisiae* results in telomere elongation. *Mol. Cell. Biol.* 9, 1488–1497.
- Schärer, O.D. (2005). DNA interstrand crosslinks: natural and drug-induced DNA adducts that induce unique cellular responses. *ChemBioChem* 6, 27–32.
- Schulz, V.P., and Zakian, V.A. (1994). The *saccharomyces PIF1* DNA helicase inhibits telomere elongation and *de novo* telomere formation. *Cell* 76, 145–155.
- Shin, J.H., and Kelman, Z. (2006). DNA unwinding assay using streptavidin-bound oligonucleotides. *BMC Mol. Biol.* 7, 43.
- Sikorski, R.S., and Hieter, P. (1989). A system of shuttle vectors and yeast host strains designed for efficient manipulation of DNA in *Saccharomyces cerevisiae*. *Genetics* 122, 19–27.
- Singh, D.K., Popuri, V., Kulikowicz, T., Shevelev, I., Ghosh, A.K., Ramamoorthy, M., Rossi, M.L., Janscak, P., Croteau, D.L., and Bohr, V.A. (2012). The human RecQ helicases BLM and RECQL4 cooperate to preserve genome stability. *Nucleic Acids Res.* 40, 6632–6648.
- Stavropoulos, D.J., Bradshaw, P.S., Li, X., Pasic, I., Truong, K., Ikura, M., Unguin, M., and Meyn, M.S. (2002). The Bloom syndrome helicase BLM interacts with TRF2 in ALT cells and promotes telomeric DNA synthesis. *Hum. Mol. Genet.* 11, 3135–3144.
- Studier, F.W. (2005). Protein production by auto-induction in high density shaking cultures. *Protein Expr. Purif.* 41, 207–234.
- Suzuki, T., Kohno, T., and Ishimi, Y. (2009). DNA helicase activity in purified human RECQL4 protein. *J. Biochem.* 146, 327–335.
- Tang, G., Peng, L., Baldwin, P.R., Mann, D.S., Jiang, W., Rees, I., and Ludtke, S.J. (2007). EMAN2: an extensible image processing suite for electron microscopy. *J. Struct. Biol.* 157, 38–46.
- Teng, S.-C., and Zakian, V.A. (1999). Telomere-telomere recombination is an efficient bypass pathway for telomere maintenance in *Saccharomyces cerevisiae*. *Mol. Cell. Biol.* 19, 8083–8093.
- Teng, S.-C., Chang, J., McCowan, B., and Zakian, V.A. (2000). Telomerase-independent lengthening of yeast telomeres occurs by an abrupt Rad50p-dependent, Rif-inhibited recombinational process. *Mol. Cell* 6, 947–952.
- Tomasz, M. (1995). Mitomycin C: small, fast and deadly (but very selective). *Chem. Biol.* 2, 575–579.
- Ward, T.A., Dudášová, Z., Sarkar, S., Bhide, M.R., Vlasáková, D., Chovanec, M., and McHugh, P.J. (2012). Components of a Fanconi-like pathway control Pso2-independent DNA interstrand crosslink repair in yeast. *PLoS Genet.* 8, e1002884.
- Wellinger, R.J., and Zakian, V.A. (2012). Everything you ever wanted to know about *Saccharomyces cerevisiae* telomeres: beginning to end. *Genetics* 191, 1073–1105.
- Wu, Y., and Brosh, R.M., Jr. (2010). Helicase-inactivating mutations as a basis for dominant negative phenotypes. *Cell Cycle* 9, 4080–4090.
- Zhou, J.-Q., Monson, E.M., Teng, S.-C., Schulz, V.P., and Zakian, V.A. (2000). The Pif1p helicase, a catalytic inhibitor of telomerase lengthening of yeast telomeres. *Science* 289, 771–774.
- Zhu, Z., Chung, W.H., Shim, E.Y., Lee, S.E., and Ira, G. (2008). Sgs1 helicase and two nucleases Dna2 and Exo1 resect DNA double-strand break ends. *Cell* 134, 981–994.